

Arrays of two-state stochastic oscillators: Roles of tail and range of interactions

Alexandre Rosas*

Departamento de Física, CCEN, Universidade Federal da Paraíba, Caixa Postal 5008, 58059-900, João Pessoa, Brazil

Daniel Escaff

Complex Systems Group, Facultad de Ingeniería y Ciencias Aplicadas, Universidad de los Andes, Avenida Moseñor Álvaro del Portillo No. 12.455, Las Condes, Santiago, Chile

Italo'Ivo Lima Dias Pinto

Laboratório de Física Teórica e Computacional, Departamento de Física, Universidade Federal de Pernambuco, 50670-901 Recife, PE, Brazil

Katja Lindenberg

Department of Chemistry and Biochemistry, and BioCircuits Institute, University of California San Diego, La Jolla, California 92093-0340, USA

(Received 21 November 2016; published 2 March 2017)

We study the role of the tail and the range of interaction in a spatially structured population of two-state on-off units governed by Markovian transition rates. The coupling among the oscillators is evidenced by the dependence of the transition rates of each unit on the states of the units to which it is coupled. Tuning the tail or range of the interactions, we observe a transition from an ordered global state (long-range interactions) to a disordered one (short-range interactions). Depending on the interaction kernel, the transition may be smooth (second order) or abrupt (first order). We analyze the transient, which may present different routes to the steady state with vastly different time scales.

DOI: [10.1103/PhysRevE.95.032104](https://doi.org/10.1103/PhysRevE.95.032104)**I. INTRODUCTION**

Emergent behaviors of systems that consist of many coupled constituent units have captured the attention of the scientific community for decades. Examples of this kind of behavior can be found in many contexts, starting from equilibrium phase transitions [1]. Traditional examples go from equilibrium magnetic systems that have become paradigmatic of how their constituents (up-down spins) can be in an ordered state other than randomly evenly distributed up and down, to more complex nonequilibrium transitions such as synchronization [2–4], where many nonlinear oscillators are able to oscillate in unison. The key to understanding these processes begins with the interactions that might allow the units to display their dynamics in a coordinated way.

Many theoretical models have been used to describe such dynamics. Here we focus on systems whose units have a discrete number of states, with Markovian rate processes governing transitions between these states. Such dynamics have traditionally been used to model processes in physics and chemistry [5–7], and in recent years they have also been applied to ecology and to problems in the social sciences. For instance, Kirman [8] used this approach to simultaneously address two distinct but closely related problems: how ants decide between two different but identical sources of food, and how consumers decide between two different but in some sense equivalent products. Each of these problems was modeled as a Markov chain of interacting units, each of which could

be in one of two states (i.e., spinlike). In both cases, the majority of the population prefers one of the two states, but this preference can switch stochastically to the other state. This explains switching as a stochastic phenomenon rather than one that relies on multiple equilibria, and it is in agreement with observations in entomology and in economics. Spinlike models for situations involving decisions have become a fruitful field of research [9]. A paradigmatic example is the voter model [10], which has expanded to include many situations, such as the addition of stubborn voters or even agents that do not change their opinions (zealots) [11,12], and contrarian agents [13]. Among many examples, the voter model has also been used in small-world networks [14] and in heterogeneous graphs [15,16]. Beyond the social sciences, this modeling approach has been used in population genetics [17] and in ecology [18,19]. Here, we will consider two-state units (on-off units) as a simple abstract dynamics without a claim of specific applicability.

Wood *et al.* [20–23] have proposed a three-state model that exhibits an interesting transition to synchronization. When uniform global coupling is considered, the system synchronizes due to Hopf bifurcation (i.e., a second-order phase transition) to a state in which the units tend to oscillate in unison. By “uniform global coupling” we mean all-to-all coupling all of equal strength. In a particular rendition of the model, further increasing the coupling strength leads to a slowing down of the state-to-state transitions until the oscillatory global state is lost altogether via an infinite-period bifurcation [24,25], and the system reaches a static stationary state in which most of the units are locked and static in the same state. Note that with uniform global coupling, we do

*arosas@fisica.ufpb.br

not introduce the notion of dimensionality, nor do we need to address any “spatial” questions. One simply deals with the global densities of units in each state.

Beyond global coupling, Wood *et al.* have explored local coupling [20,21], that is, the placement of three-state Markovian units on a regular lattice with nearest-neighbor interactions. Under these conditions, it is of course necessary to include “dimensionality” and “space” in the discussion. The system is able to synchronize to global oscillatory behavior only in three or more spatial dimensions. Therefore, the lower critical dimension to observe oscillatory synchronization is $d = 2$.

Later it was shown that when nonlocal (but not uniform global) interactions with more distant neighbors are considered, the system is able to synchronize with sufficiently distant and strong interactions even in one dimension [26]. Furthermore, with appropriate nonlocal interactions, the lattice exhibits new self-organized behaviors such as wave formation in a parameter regime where no synchronous behavior of any kind is observed for a globally coupled system. Spatial patterning has also been documented for similar models in the context of population genetics [27].

Two-state models with Markovian intra-unit transition rates are simpler to analyze, but with our form of coupling, a transition to oscillatory behavior is not possible regardless of the coupling strength. Transitions to motionless ordered phases in which the fraction of oscillators in each state is not $1/2$ even if the potential shows no asymmetry, on the other hand, are possible, and the study of the transition to the ordered phase in uniformly globally coupled arrays can be carried out analytically, as opposed to the numerical work needed for the three-state array. In fact, uniformly globally coupled networks of two-state Markovian stochastic oscillators can even be handled analytically for finite arrays [28,29]. We can describe the transition to an ordered phase taking into account the fluctuations induced by the finite size of the system via a Fokker-Planck equation, with an exact solution for the steady-state distribution. Similar approaches have been used in the context of the voter model [13], and exact results have been obtained in the presence of external perturbations [30]. We note that when non-Markovian effects (memory) are introduced into intra-unit transitions in our model, oscillatory behaviors may be observed even for two-state globally coupled networks [31,32].

The purpose of this paper is to explore the transition to an ordered phase in a two-dimensional lattice of two-state Markovian units with local or nonlocal interactions, including interactions whose strength may depend on distance. This means that dimensionality and location must now be included in the analysis – it is not sufficient to address only global mean-field densities of oscillators in one state or the other. We pose the following question: what is the necessary distance dependence and range of interactions that will lead to ordered behavior, that is, to stationary states where there are more units in one state than in the other even with no inherent potential asymmetry?

We choose two models. In one, which we call the “long-tail model”, we assume a power-law dependence of the transition rates on the distance of each given unit on the states of its neighbors. For this model, we look for the highest degree of

the polynomial that still allows the phase transition for a given interaction strength parameter. (If the degree of the polynomial were zero, we would be back to uniform global coupling, while a very high degree strongly limits the range of interactions and brings us back to the local picture.) Our second model, which we call the “uniform kernel model”, is akin to a hat, where the interaction of each given unit with its neighbors is uniform up to a given range, beyond which it abruptly falls to zero. Here we explore the distance of interactions needed for a given interaction strength. In both cases, our control parameter is the interaction strength. We also explore the order of the transition to order in both cases (to compare with the second-order transition in the uniformly globally coupled model).

Our presentation is organized as follows. In Sec. II we review our uniform global coupling theory and present our two models. In Sec. III we present our results for the phase transitions to an ordered phase for each model. Interesting findings include the transient behaviors on the way to the stationary states, the phase diagrams of the stationary states, and the nature of the transitions from disordered to ordered stationary states. In Sec. IV we present a brief summary and some concluding remarks.

II. THE MODEL

We consider a two-dimensional square lattice, where the position of a unit in the array is indicated by the vector $\vec{k} \in \{(k_x, k_y)\}_{k_x, k_y=1}^L$. The total number of units is then $N = L^2$. The basic unit of our model is a two-state (0 and 1) Markovian oscillator. We denote the state of the oscillator at position \vec{k} by the binary indicator $s_{\vec{k}}(t) \in \{0, 1\}$. The oscillator transitions from state 0 to state 1 occur with a transition rate γ_0 , and from state 1 to state 0 with a transition rate γ_1 .

The interaction between units is modeled via a dependence of the rates γ_0 and γ_1 on the states of all the neighbors with which each given unit interacts. More precisely, at each position in the array we define

$$v_{\vec{k}}(t) = \sum_{\vec{k}'} f(\vec{k}') s_{\vec{k}+\vec{k}'}(t), \tag{1}$$

where the sum is over the entire square lattice, with periodic boundary conditions, and f is a normalized kernel function that accounts for the range of the interaction,

$$\sum_{\vec{k}} f(\vec{k}) = 1. \tag{2}$$

Then the transition rates of the unit at location \vec{k} now depend on $v_{\vec{k}}$,

$$\gamma_0 \rightarrow \gamma_0(v_{\vec{k}}) \text{ and } \gamma_1 \rightarrow \gamma_1(v_{\vec{k}}). \tag{3}$$

A. All-to-all interactions of uniform strength

To better place our two models in context, we first consider an all-to-all interaction of uniform strength, that is, a kernel function

$$f(\vec{k}) = \frac{1}{L^2} = \frac{1}{N}. \tag{4}$$

Consequently, we have

$$v_{\vec{k}}(t) = \frac{1}{N} \sum_{\vec{k}'} s_{\vec{k}'}(t) = n_1(t), \quad (5)$$

where $n_1(t)$ is the global density of oscillators in state 1. Therefore, the position dependence is no longer relevant,

$$\gamma_0 \rightarrow \gamma_0(n_1) \text{ and } \gamma_1 \rightarrow \gamma_1(n_1). \quad (6)$$

In the thermodynamic limit $N \rightarrow \infty$, the evolution of the global density is described by the differential equation

$$\dot{n}_1 = F(n_1) = \gamma_0(n_1)(1 - n_1) - \gamma_1(n_1)n_1. \quad (7)$$

In this limit, there are no finite-size fluctuations, so we can call on the mean-field relationship between the global density, the mean global density, and the probability of finding a unit in state 1 at time t ,

$$\lim_{N \rightarrow \infty} n_1 = \langle n_1 \rangle = P_1. \quad (8)$$

Equation (7) is then also the master equation for the probability $P_1(t)$. To describe the second-order transition from disorder to order, note that Eq. (7) has the form

$$\dot{n}_1 = -\frac{\partial \mathcal{U}_{\text{MF}}}{\partial n_1}, \quad (9)$$

where $\mathcal{U}_{\text{MF}} = -\int_0^{n_1} F(n)dn$ is a mean-field potential. Therefore, Eq. (7) dictates a relaxation dynamics that tends to minimize \mathcal{U}_{MF} .

We introduce the symmetric potential that we have introduced in our earlier studies [28,29],

$$\mathcal{U}_{\text{MF}}(n_1) = \frac{1}{4}[\varepsilon - (n_1 - 1/2)^2]^2, \quad (10)$$

which models a transition from disorder to order, as we move the control parameter ε . For $\varepsilon < 0$, the minimum energy corresponds to the disordered phase, $n_1 = 1/2$, where half of the units are in state 1 and the other half are in state 0. When $\varepsilon > 0$, the disordered state corresponds to a maximum of the potential Eq. (10), which then exhibits two new minima at $n_{\pm} = 1/2 \pm \sqrt{\varepsilon}$. These phases are ‘‘ordered’’ states, where more than half of the units are in the same state. The transition from disorder to order is continuous (second order). The maximum possible value of the control parameter is $\varepsilon = 1/4$, at which point all the units are in the same state. We exclude values $\varepsilon > 1/4$ since these would place the minima n_{\pm} outside of the physically permissible range $0 < n_1 < 1$.

We associate the double-well potential Eq. (10) with the transition rates

$$\gamma_0(n_1) = \frac{1}{2}n_1^2 + \frac{1 - 4\varepsilon}{8}, \quad (11)$$

$$\gamma_1(n_1) = \frac{1}{2}(1 - n_1)^2 + \frac{1 - 4\varepsilon}{8}, \quad (12)$$

which satisfy the symmetry $\gamma_0(n) = \gamma_1(1 - n)$. Note that the requirement that these rates be positive also excludes values $\varepsilon > 1/4$.

As we showed in Ref. [28], for large but finite N the deterministic evolution equation (7) for the global density must be augmented by finite-size fluctuations. The appropriate

description is now the Langevin equation

$$\dot{n}_1 = F(n_1) + \sqrt{\frac{G(n_1)}{N}}\xi(t), \quad (13)$$

where $F(n_1)$ coincides with the mean-field force of Eq. (7), and $\xi(t)$ is white Gaussian zero-centered δ -correlated multiplicative noise, with

$$G(n_1) = \gamma_0(n_1)(1 - n_1) + \gamma_1(n_1)n_1. \quad (14)$$

In the thermodynamic limit, $N \rightarrow \infty$, the last term on the right-hand side of Eq. (13) vanishes and the equation reverts to the deterministic form. Note the appropriate $N^{-1/2}$ dependence of the additional term on the system size.

Interpreting Eq. (13) in the Itô sense leads to the Fokker-Planck equation for the probability $P(n_1, t)$ that the fraction of units in state 1 is equal to n_1 at time t ,

$$\begin{aligned} \frac{\partial}{\partial t} P(n_1, t) = & -\frac{\partial}{\partial n_1} [F(n_1)P(n_1, t)] \\ & + \frac{1}{2N} \frac{\partial^2}{\partial n_1^2} [G(n_1)P(n_1, t)]. \end{aligned} \quad (15)$$

The steady-state probability, that is, the stationary solution of the Fokker-Planck equation, is then

$$\mathcal{P}_{\text{st}}(n_1) = C \frac{\exp[-2N\mathcal{U}_{\text{eff}}(n_1)]}{G(n_1)}, \quad (16)$$

where C is the normalization constant, and

$$\mathcal{U}_{\text{eff}}(n_1) = -\int_0^{n_1} \frac{F(n)}{G(n)} dn. \quad (17)$$

Therefore, for large enough N , the most likely states correspond to the minima of potential Eq. (17). Although this potential is modified from the potential Eq. (10) due to the finite-size effects, the minima of the two potentials coincide at $F(n_1) = 0$. We note that in contrast with our previous work [28,29], the choices of $F(n_1)$ and $G(n_1)$ in the Langevin equation (13) ensure that the transition rates to/from the two states are symmetric, that is, the fluctuations do not add a bias to one or the other state.

B. Interactions of variable strengths

We now move away from uniform global interactions to our models that require nonuniform kernel functions $f(\vec{k})$; cf. Eqs. (1) and (2). Here we introduce two different kernels. The first is a long-tailed kernel describing interactions that decrease with distance as an inverse power of the distance between units:

$$f(\vec{k}) = \frac{N_n}{(1 + k^2)^n}, \quad (18)$$

where N_n is a normalization constant and n controls the tail of the interaction kernel. For small n the decay of the interaction kernel is slow, so we expect behavior similar to that of the uniform global coupling model. As n increases, the interaction becomes more and more local. For sufficiently large values of n , we expect the behavior of uncoupled oscillators with no phase transition to order.

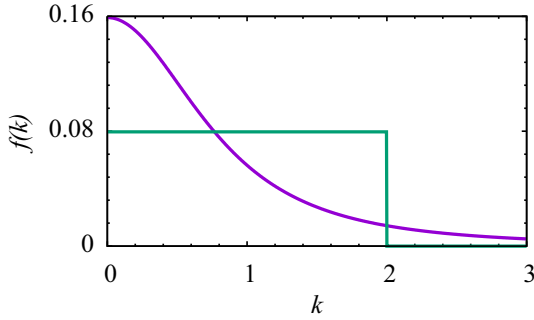


FIG. 1. Dependence of the two kernels on distance. In this figure, we used $n = 1.5$ (smooth curve) and $\sigma = 2.0$ (rectangular curve). The comparison is qualitative, not quantitative, in this figure.

The second is a uniform local kernel,

$$f(\vec{k}) = \begin{cases} N_\sigma & \text{for } k < \sigma, \\ 0 & \text{otherwise.} \end{cases} \quad (19)$$

Here N_σ is also a normalization constant and σ determines the range of the interaction. For small σ , we expect the oscillators to remain disordered, while for large σ we anticipate behavior similar to the uniform global coupling model.

These two kernels allow us to separate and analyze different qualitative aspects of the problem. While both kernels can go from a local to an all-to-all interaction, they do so in different ways. The long-tailed kernel reveals the importance of the form of the decay of the interaction for the evolution of the system, while the uniform kernel focuses exclusively on the range of the interaction. The different behaviors of the two kernels are qualitatively illustrated in Fig. 1. Both kernels obey the proper normalization Eq. (2), but the areas in the figure need to be adjusted with the appropriate numbers of neighbors to achieve this normalization.

C. Spatially extended mean-field theory

It is convenient to reformulate this problem from a discrete version to a continuous one. This approach was used successfully in our earlier work in [26] for a one-dimensional array of three-state units interacting with the kernel function Eq. (19). The same approach can be used here for two-state units interacting with an arbitrary kernel function in two spatial dimensions. It is a mean-field approach that starts with transforming the lattice into a continuous square, with

$$\vec{k} \rightarrow \vec{x} \in \mathcal{C}_1 = [0, 1] \times [0, 1]. \quad (20)$$

Here $\vec{x} = \vec{k}/L$ and $dx = L^{-1}$. Next we implement the mean-field approximation

$$v_{\vec{k}}(t) \approx v(\vec{x}, t) = \int_{\mathcal{C}_1} f(\vec{x}') p_1(\vec{x} + \vec{x}', t) d^2 x', \quad (21)$$

where $p_1(\vec{x}, t)$ is the probability density for the unit at position \vec{x} to be in state 1 at time t . This probability density obeys the equation

$$\begin{aligned} \frac{\partial p_1(\vec{x}, t)}{\partial t} &= \gamma_0(v(\vec{x}, t))(1 - p_1(\vec{x}, t)) \\ &\quad - \gamma_1(v(\vec{x}, t))p_1(\vec{x}, t), \end{aligned} \quad (22)$$

which is the generalization of Eq. (7) to include spatial location.

Equation (22) does not predict steady-state pattern formation [27, 33–36], nor does it yield the formation of permanent defects [37–41], as do similar descriptions in other systems. However, as we show in the next section, we find a remnant of sorts of these behaviors. We show that the system displays a domain dynamics, often called coarsening, similar to the genetic invasion observed in population genetics in the case of disruptive selection [27]. We will see that for $\varepsilon > 0$, that is, for ε above the mean-field critical point, we obtain results that can be described as a two-step process, one that occurs on a fast time scale and a second on a much slower time scale. In the first, the system produces large local domains where one of the two “ordered” states, $p_1 = n_+ = 1/2 + \sqrt{\varepsilon}$ or $n_- = 1/2 - \sqrt{\varepsilon}$, clearly dominates. On the slow time scale, we observe domain dynamics (frequently called coarsening dynamics) aimed at establishing a global equilibrium that consists of a completely uniform state with $p_1 = n_+$ or n_- in the entire square. We next present numerical results quantifying and confirming this description, and we also elucidate the nature of the phase transition from disorder to order for each model.

III. RESULTS

We carried out simulations of our models on 512×512 lattices with $\varepsilon = 0.22$ except where otherwise indicated. The neighborhoods of all the units that contribute to our results were circles of radius $L/2$ ($L = 512$), and we used periodic boundary conditions. The finite size of the lattice is sufficiently large so that it does not introduce strange unphysical effects, that is, the lattice is large enough so that its finite size does not introduce spurious results, and the contributions of the interactions across long distances are negligible. We tested larger lattices and saw no changes in our results (except for the occurrence of longer transients; see below). We started from two types of initial conditions: all the oscillators in one state (uniform initial condition), and the states of the oscillators randomly chosen with equal probability (random initial condition). These two initial conditions are close to one or the other steady state of the globally coupled model.

A. Steady state

1. Long-tail model

For the kernel function Eq. (18) with small n (long tails), the oscillators approach the distributions of the globally coupled model. As n increases and the interaction becomes more and more local, the system smoothly becomes uncoupled. In Fig. 2, we show the steady-state density of the less populated state d_l as a function of n . We choose to present d_l instead of the density of one of the two populations because each sample is equally likely to arrive at a state where one or the other population is dominant. Therefore, averaging the density of one population over different samples would lead to meaningless results. The transition is smooth albeit rapid, i.e., it is a second-order transition.

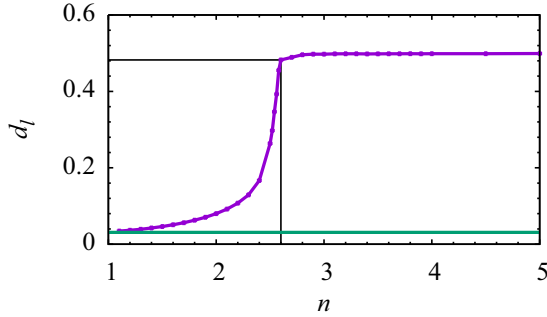


FIG. 2. Steady-state density of the less populated state (averaged over 10 samples) as a function of n (purple) for the long-tail model. The horizontal (green) line is the lower stable steady-state density in the globally coupled model.

The spatial structure brings a new feature into the model not present in the globally coupled model, namely the appearance of density fluctuations (see Fig. 3). We ascertained that the fluctuations in Fig. 3 are not finite-size effects by comparing the simulation on a lattice of 512×512 sites with one on a lattice of 2048×2048 sites and seeing essentially the same distributions. Since finite-size fluctuations depend on lattice size, these two distributions would be different. Also, finite-size fluctuations in Fig. 3 would scale as $\sim 1/N = 1/512 = 0.002$, that is, orders of magnitude smaller than those visible in the figure. Note that the choice of n in this figure places the system at the start of the regime of the random steady state; cf. Fig. 2.

To quantify these density fluctuations further, we divided the lattice into $N_l = (L/l)^2$ boxes of side l and computed the density in each box. Next we defined the parameter $\tilde{\Delta}$ as the mean-square deviation of the density of the boxes from

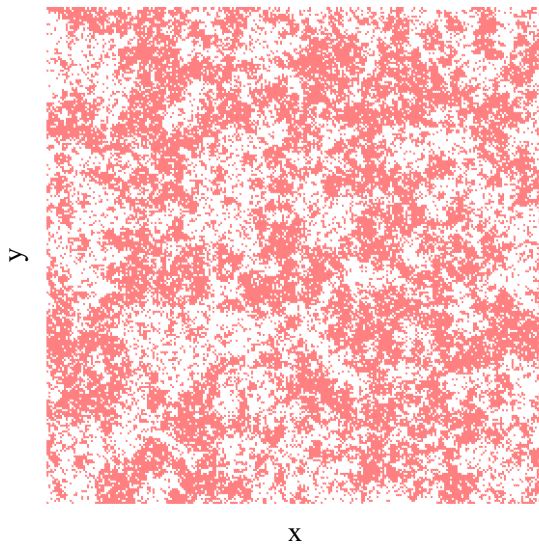


FIG. 3. Snapshot of the steady state (4000 time units after the start of the simulation) for $n = 2.6$. The oscillators in state 0 are represented by red dots, and those in state 1 are represented by white dots. The simulation is over a lattice of 512×512 two-state units; the figure shows 1/4 of the lattice, namely a 256×256 portion.

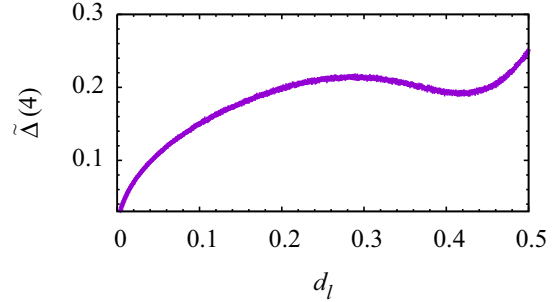


FIG. 4. Parameter $\tilde{\Delta}$ for random samples as a function of the density of the less populated state in the long-tail model. The reason for the nonmonotonic behavior is not obvious.

the lattice density,

$$\tilde{\Delta}(l) = \frac{1}{N_l} \sum_{k=1}^{N_l} (n_1^{(k)} - n_1)^2. \quad (23)$$

The parameter $\tilde{\Delta}$ would vanish for a completely uniform distribution and is nonzero for a random distribution (see Fig. 4). The parameter increases as fluctuations increase. Here we wish to quantify the density fluctuations due to the model and not those due to a given distribution. A better choice to quantify those purely due to the model is to define a new parameter Δ that subtracts the effect of the random fluctuations from $\tilde{\Delta}(l)$,

$$\Delta(l) = \tilde{\Delta}(l) - \tilde{\Delta}_R(l), \quad (24)$$

where the subscript R stands for random sample. To calculate Δ_R for a given density n_1 , we randomly distribute $n_1 \times L^2$ units in state 1 on an $L \times L$ lattice and the remaining oscillators in state 0. We calculate the value of $\tilde{\Delta}(l)$ according to Eq. (23) for this lattice, and we average this value of $\tilde{\Delta}$ for many samples. This average value is $\tilde{\Delta}_R(l)$. Figure 5 shows this parameter as a function of n . As we can see, the density fluctuations are negligible for small n (because we approach the globally coupled regime) and for large values of n (because the effects of the random fluctuations in this regime have been subtracted), but they are appreciable around the transition from the globally coupled state to the uncoupled state. The appearance of fluctuations near a transition is not surprising, but cluster formation is nevertheless interesting and even unanticipated.

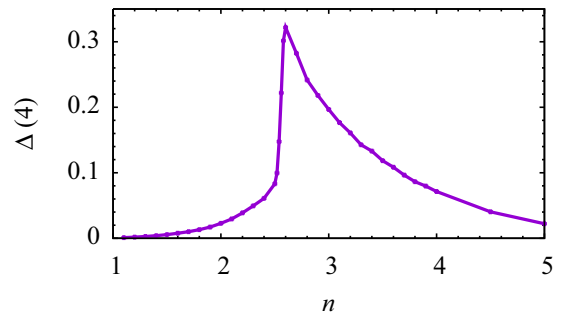


FIG. 5. Parameter $\Delta(4)$ as a function of n . See the text for a description.

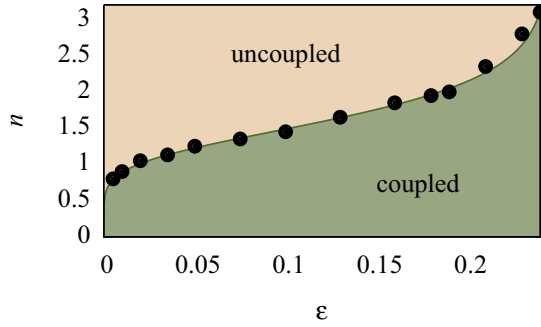


FIG. 6. Phase diagram for the long-tail model as a function of the exponent n and the parameter ε . The circles indicate the results of our simulations. We have joined the circles by a line as a guide to the eye.

Finally, in Fig. 6 we show a phase diagram for this system as a function of the exponent n and the parameter ε . The disordered steady state is associated with the uncoupled regime, and the ordered steady state is associated with the coupled regime. To decide whether to place the system in the coupled or uncoupled regime for a given pair of parameters n and ε , we start simulations from two initial conditions: one in which half of the units are in each state, and the other with all units in a single state. We let the system evolve to the steady state, which is (or should be) the same for both cases. If the steady state has half of the units in each state, we place it in the uncoupled regime; otherwise it is in the coupled regime. To deal with fluctuations, we place the system in the uncoupled regime if the fluctuations are greater than the average density of the most occupied state. We focus in particular on parameter pairs that place us at and near the boundary between the two phases.

2. Uniform kernel model

For the uniform kernel, we observe a discontinuous (first-order) transition as we increase the range of the interaction for fixed ε . If the radius of interaction is small enough so that only first neighbors interact, the system evolves to a state where almost half of the oscillators are in each state. However, even if only the next neighbors fall into the range of interactions (which corresponds to the value $\sigma \equiv \sigma_c = \sqrt{2}$), the steady-state density jumps to a value near that of the globally coupled system (see Fig. 7). While the discontinuity is caused by the discreteness of the lattice, the abrupt jump (first-order transition) is not something we foresaw. That is, due to the discreteness of the lattice, it is expected that changes in the state of the system will only occur at certain values of σ so that the number of neighbors under the influence of the interaction kernel changes. However, the abrupt change is not *a priori* obvious.

Here too in Fig. 8 we present a phase diagram as a function of the range σ and the parameter ε . The horizontal lines connecting circles for small σ are “real” in that in this regime the critical value of σ is the same for finite intervals of ε . This is a consequence of the discreteness of the lattice. Small changes in the range σ in this regime may not lead to changes in the number of neighbors. What is more, for sufficiently large

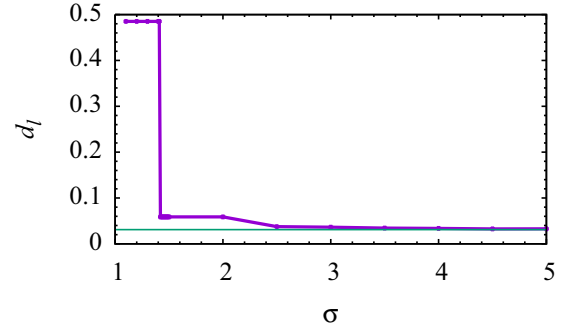


FIG. 7. Steady-state density of the less populated state as a function of σ (purple) for the uniform kernel model. The horizontal (green) line is the stable steady-state density of the globally coupled model. The first-order transition occurs at $\sigma \equiv \sigma_c = \sqrt{2}$.

values of ε (near 0.25), even nearest-neighbor interactions lead to an ordered state.

B. Transient

A uniform initial condition quickly evolves to the steady state with a very short transient. If we start with all oscillators in the same state, they will likely either evolve to an uncoupled steady state or to a steady state with a larger prevalence of oscillators in the initial state, depending on the range of interaction (σ) or the tail of the distribution (n). This evolution ends quickly. However, when we start the system with half of the oscillators in each state and the interaction between the oscillators is strong enough (small n , large σ), there is a competition between the two possible steady states. The system may evolve to the final state with a larger prevalence of one or the other state with equal probability. However, this competition leads to the formation of large domains of the two possible steady states that compete. Ultimately, one domain wins the battle, but the evolution may be very slow and the transient may follow different paths.

We can group the dynamical evolution of the system to the steady state into three qualitatively different groups. The first is a trivial fast direct evolution without the formation of any large domains, as described above. This very fast equilibration typically takes about 100 units of time. The

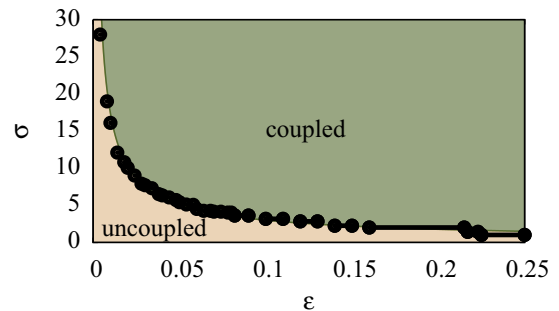


FIG. 8. Phase diagram for the uniform kernel model as a function of the range parameter σ and the parameter ε . The circles indicate the results of our simulations. We have joined the circles with a line as a guide to the eye.

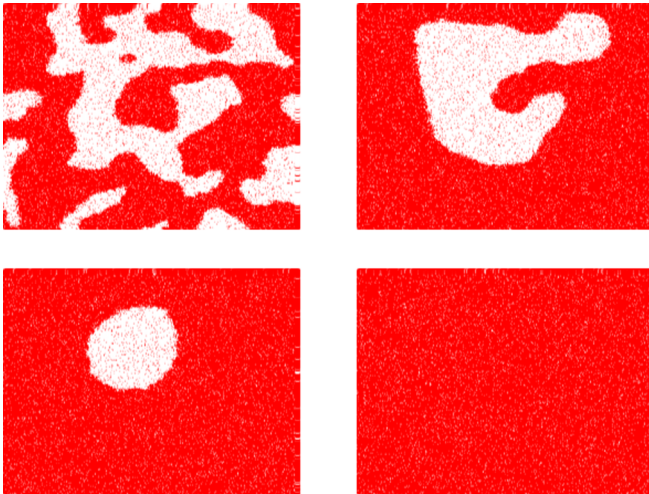


FIG. 9. Snapshots of the system configuration where large transient localized domains appear, with large regions of one state surrounding interior domains of the other. The four panels left to right and top to bottom correspond to the following simulation times: $t = 500$, 2500, 9000, and 12 500. The first panel ($t = 500$) shows the early evolution, and the next one ($t = 2500$) shows a later snapshot where a large localized domain of one species is entirely surrounded by the other species. The third panel ($t = 9000$) illustrates the decrease in size of the interior domain. The final panel ($t = 12\,500$) shows the uniform stationary state, which here happens to be the “red” one. For this simulation, we used the long-tail kernel with $n = 1.6$ and a random initial condition with half of the oscillators in each state.

very early evolutions of the two other routes to the steady state are similar, but they quickly begin to differ from the fast equilibration and from each other. In both cases, we see the formation of large domains in which one or the other state is dominant (see Figs. 9 and 10). In one, the more common of the two, there appear large localized domains of mainly one state surrounded by large domains in which the other state dominates. The latter tend to extend all the way to the borders of the array, while the former are in the interior (see Fig. 9). The appearance of the large domains in the interior slows down the evolution to the steady state. Eventually the population that surrounds an interior domain encroaches inward (by causing transitions of the units in the interior domain), causing it to become smaller and smaller. The surfaces that need to be encroached become smaller and smaller, and the process speeds up until the interior domains are destroyed. The evolution to the steady state in this case typically takes from 5000 to 20 000 units of time. In the other case, the configuration in the transient regime of large domains occurs in stripes that extend throughout the lattice in one direction (see Fig. 10). This competition involves encroachment surfaces that do not decrease in size (even as the stripes of one state or the other become narrower) so that the transient dynamics to the steady state is longer, around 130 000 units of time. The reason for the slower dynamics is quite evident. In both cases, the evolution to the steady state occurs in three steps. First, on a very fast time scale, domains are created. Next, on an intermediate time scale, the curvature of the domains is smeared out. These first two steps

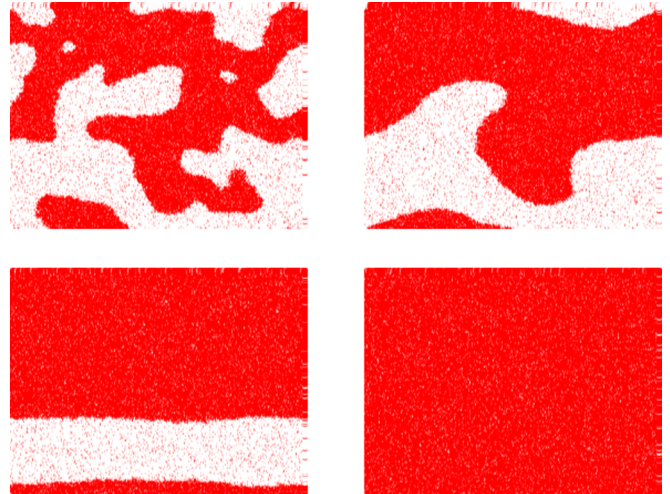


FIG. 10. Snapshots of another realization of the same system with the same parameters as in Fig. 9 but with a new initial condition. Here again large localized domains appear. The four times here are $t = 500$, 3000, 100 000, and 135 000. The first panel ($t = 500$) shows the early evolution, where it is not yet entirely clear whether stripes or interior domains will develop. The second panel ($t = 3000$) clearly shows the early evolution of a striped pattern. The third panel ($t = 100\,000$) shows neat strips with a majority of the units in the “red” state. The final panel ($t = 135\,000$) shows the uniform stationary state, which here again is the “red” state.

are very similar in both cases. However, in the stripe case we are left with an almost one-dimensional problem, while for bubble-type domains the two-dimensional characteristic of the problem causes the bubbles to disappear much more rapidly.

IV. SUMMARY AND FINAL REMARKS

In this work, we have considered arrays of two-state (“on-off”) units with Markovian transition rates between the two states. The coupling among units is reflected in the dependence of the transition rates of each unit on the states of the units to which it is coupled at the instant of the transition. The transition rates of each unit thus depend on time. In earlier work [28,29], we considered such arrays with global uniform coupling, that is, where the coupling is all-to-all and of equal strength to all. In that model, there is therefore no spatial structure.

Here we have analyzed arrays in which spatial structure plays a role in that the interactions between units depend on the distance between them in a lattice array. We have considered two different distance dependences: in one, which we call the long-tail model, the distance dependence is an inverse power law with a power-law parameter n that reflects the decay of the interaction strength with distance. A large value of n leads to a rapid decay of interaction strength with distance, while a small value indicates a slow decay, which approaches the global uniform coupling model. The second distance dependence we have considered, which we call the uniform kernel model, is one that is uniform up to a distance σ and sharply falls to zero beyond this distance. As σ increases, this model also approaches the global uniform model. However, the two models behave very differently before the global uniform

global coupling model is reached. In addition to the parameters n and σ , the two models also include an interaction strength parameter that we have called ε in both cases.

In all cases, we have considered an effective potential that has a single minimum at $n_+ = n_- = 1/2$ when $\varepsilon < 0$ and two minima at $1/2 \pm \sqrt{\varepsilon}$ when $\varepsilon > 0$. In the uniform global coupling case, the steady state at long times is either “disordered”, with half of the units randomly in one state and the other half in the other ($\varepsilon < 0$), or “ordered”, in which more than half of the units are in one of the two minima of the potential when $\varepsilon > 0$. When one starts with a disordered initial condition, the system goes to one or the other steady state depending on the value of ε , and the transition as a function of ε is smooth (second order), that is, it is a second-order transition. In the two cases considered in this paper, we have analyzed the nature of the transition from a disordered to an ordered steady state as a function of the exponent n in the long-tail model, and as a function of σ in the uniform kernel model, for a fixed value of ε . We have determined that the transition is of second order (smooth) in the long-tail model and of first order (sharp) in the uniform kernel model. We have also presented phase diagrams for both models.

The approach to the steady state presents interesting differences depending on the initial condition. When we begin with a uniform state, that is, with all units in the same state, the system evolves to the steady state, be it ordered or disordered (depending on the value of ε), in a very short time, of order of 100 time steps (all units are updated synchronously in one time step). If we are in the coupled regime as described in Figs. 6 and 8, and if the initial condition has more units in one state than in the other (“more” here meaning a difference in number greater than those associated with fluctuations), the system evolves toward an ordered steady state consisting entirely of the units initially in the majority. However, if the initial state is disordered, then the evolution to the ordered steady state is quite different. First, the system quickly evolves to a state with large domains of a majority of units in one state or the other.

This first step occurs on a time scale of about 100 time steps. Then, these domains compete with one another toward a steady state in which one or the other majority state “wins”. This evolution is slow in either model, and it may occur in two different ways. In one, smaller domains are fully surrounded by the opposite domains, which then encroach across the common boundaries. Since the common boundaries decrease in length as the encroachment continues and the inner domains become smaller and smaller, the approach to the ordered steady state speeds up until one state wins. This process occurs over approximately 5000 to 20 000 units of time. In the other, the transient domain consists of stripes of the two majority states that cross the entire system. The encroachment boundaries therefore do not decrease in length as time proceeds until one or the other disappears, and this process is therefore slower, occurring on a time scale of around 130 000 units of time. In both cases, all boundaries eventually disappear and the entire system relaxes to a single species.

In earlier work, we showed that in a two-state array no transition to order or to oscillatory behavior can occur in our approach to coupling unless at least one of the two transition rates has a memory [32]. In this work, we have dealt exclusively with Markovian transition rates, and so the ordered stationary states are static (of course with fluctuations). We have shown here that the spatial interaction structures exhibit different interesting routes to the ordered steady states, and that the tail and range of interactions bring new features to these routes that are completely absent in all-to-all uniform interaction models.

ACKNOWLEDGMENTS

D.E. thanks FONDECYT Project No. 1140128 for financial support. A.R. acknowledges Capes for its support (Grant No. 99999.000296/2015-05). K.L. acknowledges the support of the ONR under Grant No. N00014-13-1-0205.

-
- [1] K. Huang, *Statistical Mechanics* (Wiley, New York, 1987).
 - [2] S. H. Strogatz, *Physica D* **143**, 1 (2000).
 - [3] S. C. Manrubia, A. S. Mikhailov, and D. H. Zanette, *Emergence of Dynamical Order: Synchronization Phenomena in Complex Systems* (World Scientific, Singapore, 2004).
 - [4] J. A. Acebrón, L. L. Bonilla, C. J. Pérez-Vicente, F. Ritort, and R. Spigler, *Rev. Mod. Phys.* **77**, 137 (2005).
 - [5] N. Van Kampen, *Stochastic Processes in Physics and Chemistry* (Elsevier Science, Amsterdam, 1992).
 - [6] S. W. Benson, *The Foundations of Chemical Kinetics* (McGraw-Hill, New York, 1960).
 - [7] D. C. Mattis and M. L. Glasser, *Rev. Mod. Phys.* **70**, 979 (1998).
 - [8] A. Kirman, *Quart. J. Econ.* **108**, 137 (1993).
 - [9] A. Svenkeson and A. Swami, *Sci. Rep.* **5**, 14839 (2015).
 - [10] T. M. Liggett, *Interacting Particles Systems* (Springer, New York, 1985).
 - [11] E. Yildiz, A. Ozdaglar, D. Acemoglu, A. Saberi, and A. Scaglione, *ACM Trans. Econ. Comp.* **1**, 19 (2013).
 - [12] M. Mobilia, A. Petersen, and S. Redner, *J. Stat. Mech.* (2007) P08029.
 - [13] N. Masuda, *Phys. Rev. E* **88**, 052803 (2013).
 - [14] D. Vilone and C. Castellano, *Phys. Rev. E* **69**, 016109 (2004).
 - [15] V. Sood and S. Redner, *Phys. Rev. Lett.* **94**, 178701 (2005).
 - [16] V. Sood, T. Antal, and S. Redner, *Phys. Rev. E* **77**, 041121 (2008).
 - [17] M. A. M. de Aguiar and Y. Bar-Yam, *Phys. Rev. E* **84**, 031901 (2011).
 - [18] T. Butler and N. Goldenfeld, *Phys. Rev. E* **80**, 030902 (2009).
 - [19] V. Méndez, S. Fedotov, and W. Horsthemke, *Reaction-Transport Systems* (Springer-Verlag, Berlin, 2010).
 - [20] K. Wood, C. Van den Broeck, R. Kawai, and K. Lindenberg, *Phys. Rev. Lett.* **96**, 145701 (2006).

- [21] K. Wood, C. Van den Broeck, R. Kawai, and K. Lindenberg, *Phys. Rev. E* **74**, 031113 (2006).
- [22] K. Wood, C. Van den Broeck, R. Kawai, and K. Lindenberg, *Phys. Rev. E* **75**, 041107 (2007).
- [23] K. Wood, C. Van den Broeck, R. Kawai, and K. Lindenberg, *Phys. Rev. E* **76**, 041132 (2007).
- [24] V. R. V. Assis, M. Copelli, and R. Dickman, *J. Stat. Mech.* (2011) P09023.
- [25] V. R. V. Assis and M. Copelli, *Physica A* **391**, 1900 (2012).
- [26] D. Escaff, I. L. D. Pinto, and K. Lindenberg, *Phys. Rev. E* **90**, 052111 (2014).
- [27] H. Sayama, M. A. M. de Aguiar, Y. Bar-Yam, and M. Baranger, *Phys. Rev. E* **65**, 051919 (2002).
- [28] I. L. D. Pinto, D. Escaff, U. Harbola, A. Rosas, and K. Lindenberg, *Phys. Rev. E* **89**, 052143 (2014).
- [29] A. Rosas, D. Escaff, I. L. D. Pinto, and K. Lindenberg, *J. Phys. A* **49**, 095001 (2016).
- [30] D. D. Chinellato *et al.*, *J. Stat. Phys.* **159**, 221 (2015).
- [31] N. Kouvaris, F. Muller, and L. Schimansky-Geier, *Phys. Rev. E* **82**, 061124 (2010).
- [32] D. Escaff, U. Harbola, and K. Lindenberg, *Phys. Rev. E* **86**, 011131 (2012).
- [33] J. D. Murray, *Mathematical Biology* (Springer-Verlag, Berlin, 1989).
- [34] R. Lefever and O. Lejeune, *Bull. Math. Biol.* **59**, 263 (1997).
- [35] M. A. Fuentes, M. N. Kuperman, and V. M. Kenkre, *Phys. Rev. Lett.* **91**, 158104 (2003).
- [36] E. Hernandez-Garcia and C. Lopez, *Phys. Rev. E* **70**, 016216 (2004).
- [37] M. G. Clerc, D. Escaff, and V. M. Kenkre, *Phys. Rev. E* **72**, 056217 (2005).
- [38] M. G. Clerc, D. Escaff, and V. M. Kenkre, *Phys. Rev. E* **82**, 036210 (2010).
- [39] D. Escaff, *Eur. Phys. J. D* **62**, 33 (2011).
- [40] C. Fernandez-Oto, M. G. Clerc, D. Escaff, and M. Tlidi, *Phys. Rev. Lett.* **110**, 174101 (2013).
- [41] D. Escaff, C. Fernandez-Oto, M. G. Clerc, and M. Tlidi, *Phys. Rev. E* **91**, 022924 (2015).